6.3 **A COMPARISON OF HIGH RESOLUTION TORNADO SURVEYS TO DOPPLER RADAR OBSERVED VORTEX PARAMETERS: 2011-2012 CASE STUDIES**

James G. LaDue[1]*, Kiel Ortega[2,3], Brandon Smith[2,3], Greg Stumpf[2,3], and Darrel Kingfield[2,3]
[1]NOAA/NWS/OCWWS/Warning Decision Training Branch (WDTB), Norman, OK
[2]NOAA/OAR/National Severe Storms Laboratory (NSSL), Norman, OK
[3]Cooperative Institute for Mesoscale Meteorological Studies (CIMMS), Norman, OK

1. INTRODUCTION

We are motivated to the goal of mitigating negative outcomes from specific hazards like tornadoes as a result of findings from recent NWS service assessments. These findings revealed that warning responses were often inadequate, sometimes due to lack of specific information regarding the magnitude of the threat and expected impacts (NOAA, 2011a & b). As a response, the Central Region of the NWS initiated an impact-based tornado warning experiment in 2012 (Hudson et al. 2012b). Forecasters were expected to disseminate tiered tornado warnings based on the potential damage they may cause. Though nowcasting tornado intensity wasn't explicitly included in the directives for the experiment, forecasters still based their impact-based warnings (K. Cook 2012, personal communication) and evaluations (Hudson et al. 2012a) on intensity. However, to the author's knowledge, no published guidance was available for forecasters to nowcast intensity.

To produce this guidance we need to know if there is a relationship between the most common attributes of tornado signatures in the WSR-88D and the observed strength of the tornado. Currently, multiple methods are being applied to evaluate this relationship. For example, Toth et al. (2011) compared maximum tornado intensity estimated by mobile, near-range radar to the maximum low-level velocity difference (LLDV) in the WSR-88D vortex signature. Smith et al. (2012) manually related the maximum tornado rating to the maximum WSR-88D LLDV and near storm environmental parameters within 40 km grid boxes. Kingfield et al. (2012) also used the maximum tornado rating from track segments in Storm Data; however they chose a thorough comparison to multiple intensity-based Mesocyclone Detection Algorithm (MDA) attributes. All three studies compared the maximum tornado intensity from its entire lifespan, or at least a significant portion of it. However, an impact-based tornado warning requires a real-time nowcast of tornado intensity. This study builds upon the work of Kingfield et al. (2012) and attempts to answer whether a radar-based real-time nowcast is possible. Then contingent on a positive answer, guidance can be developed based on a more thorough study.

* *Corresponding Author Address:* James G. LaDue, NOAA/NWS Warning Decision Training Branch, 120 David L. Boren Blvd., Norman, OK, 73072; e-mail: james.g.ladue@noaa.gov.

2. BACKGROUND

2.1 Radar

The major challenge to making a successful relationship between observed and radar-based tornado intensity is beam center offset relative to a vortex center. Just the variance of this offset, in addition to other noise sources, can create a random distribution of vortex strengths measured by velocity difference of the vortex signature. So to perceive a real change in vortex strength, Wood and Brown, 1997 found that the signature strength would have to overwhelm the uncertainty introduced by beam registration. At the time of their study, the WSR-88D was operating with a roughly 1.4° effective beam width.

Now the advent of the super-resolution data has reduced the effective beam width to nearly 1° (Torres and Curtis, 2007). Thus the sampling of WSR-88D vortex signatures has improved (Brown et al. 2005) and the scan-to-scan uncertainty in strength should have diminished.

2.2 Verification

High-resolution ground truth is a necessity to evaluate tornado intensity at small temporal increments. Storm Data cannot be used since it only documents one rating for an entire tornado path (NOAA, 2007). In addition, only one width entry is placed for the tornado. High-resolution track data has only been created for special events either from major outbreaks (e.g., Speheger et al. 2002) or from field projects (e.g., Wurman and Alexander, 2005). To date, only a few studies (e.g., Burgess et al. 2002) have been able to compare WSR-88D vortex signature strength to high-resolution tornado surveys such as those documented by Speheger et al. (2002).

Storm surveying has been on the cusp of major improvements in resolution in the last two years. First, the EF-scale has been introduced (WSEC, 2006) allowing surveyors to utilize a greater variety of damage indicators. In addition, an NWS team has created a storm Damage Assessment Tool (DAT; Fig. 1) allowing for a much greater efficiency in generating high-resolution damage surveys (Stellman and Camp, 2012). After two years of use and a large number of tornadoes, the number of high-resolution tornado surveys dramatically increased.

3. METHODOLOGY

3.1 User-defined vortex identification

To create scan-by-scan comparisons, we employed a similar method to Burgess et al. (2002). Level-II data was displayed along with tornado track data and the vortex signature was located to be most likely associated with the track. As an example, the track displayed in figure 2 is from the Reform to Cordova, AL, tornado from 27 April 2012.

Displaying uncorrected velocity data was especially useful in that a proper dealiasing could be done (Fig. 3). Then the low-level velocity difference between the velocity extrema was calculated, and we documented the location of the vortex core (between the velocity extrema). Note that we included vortices that had isolated velocity peaks closest to the tornado path. No velocity extrema were used that did not appear to be associated with the tornado.

3.2 Tornado intensity

The tornado strength was determined by isolating the section of track closest to the time of the lowest elevation velocity scan. Typical tornado tracks from the DAT include a polygon enclosing the EF0 damage, and additional EF-scale contours (Fig. 4). The individual Damage Indicators (DIs) also help to verify the confidence of the tornado intensity. Aerial imagery provided additional help in either confirming the survey or by making adjustments where damage to DIs obviously fell outside of the ± one EF-scale using an application of Brown (2010). The imagery was made available via the National Geodetic Survey of NOAA and has a comparable resolution to the imagery used in Brown (2010).

The maximum EF-scale rating was found within a spatial window converted from a ±2 minute window of the user-defined vortex time and location using the vortex motion determined by radar (Fig. 5). The maximum reliable EF-scale found in this window was applied to the time of the lowest elevation scan start time. In this example, several DI's had EF3 damage within this window. We also documented the closest distance from the tornado center (yellow line normal to tornado motion) to the user identified vortex location from the WSR-88D. The same step was done for the Tornado Detection Algorithm (TDA; Mitchell et al. 1998) and Mesocyclone Detection Algorithm (MDA; Stumpf et al. 1998) locations. If the user identified vortex center was within the axis of the most intense damage (highest EF-scale) the distance was set to zero.

3.3 MDA and TDA matching

MDA and TDA detections were selected that fall within 5 km of the tornado location. If more than one MDA or TDA detection satisfies this window, then the strongest of each is preserved. This matching procedure is similar to that of Kingfield et al. (2012) except for this case the tornado location has been manually identified as mentioned in 3.2.

4. RESULTS

In our results, we sampled tornadoes from two major tornado outbreaks (2011 April 27, 2011 May 24) and three smaller events (Table 1). Fifteen tornadoes were sampled, 11 of them from supercells and the rest from QLCS events. In all, there were 179 scans selected in which there was a user-defined vortex signature at the lowest elevation angle containing an isolated V_{max} and V_{min}. Of those scans there were 100 MDA detections and 150 TDA detections. A manual inspection of failed MDA detections revealed that there was a potential lack of enough pattern vectors (Stumpf et al. 1998) to identify mesocyclones due to either dealiasing errors or the structure of the vortices did not approximate Rankine Combined Vortices.

Specific case studies of tornadoes show a diversity of relationships between LLDV and EF-scale. The Cullman, AL, tornado shown in figure 6 shows a relatively good relationship between the user-defined LLDV and EF-scale everywhere except at the first scan where isolated EF4 damage was found in downtown Cullman despite a relatively low LLDV of 70 ms^{-1}. The tornado otherwise exhibited mostly EF2-3 strength and strengthened as the user-defined LLDV correspondingly increased to 90 ms^{-1} as the longest swath of EF4 damage occurred in this tornado. As the tornado weakened for the final time, the user-defined LLDV gradually decreased to 60 ms^{-1} and then finally to less than 50 ms^{-1} when only EF0 damage was observed.

Not all tornadoes showed such a good relationship. The Tuscaloosa tornado began with very high user-based vortex LLDV (120 ms^{-1}) as high-end EF4 damage was reported just east of Tuscaloosa (Fig. 7) according to Stefkovich et al. 2012. But the user-defined LLDV slowly decreased, lowering to 80 ms^{-1} when the tornado again produced EF4 mainly over Concord, AL. The second intensification period was coincident with a smaller diameter, however, but other issues may be disassociating the relationship between the user-defined LLDV. One of these may have been that the radar was no longer viewing the radial component of the tornado's motion and therefore may not have been detecting the strong track-parallel flow to the right of the tornado. Another may have been the weakening relationship between the strength of the parent mesocyclone and tornado. However, the reflectivity debris ball (Bunkers and Baxter, 2011) was as pronounced as it was with the tornado east of Tuscaloosa.

For both the Cullman and Tuscaloosa tornadoes (Figs. 6 and 7 respectively), there was a weaker subjective relationship between the EF-scale rating and the MDA and TDA LLDV. The MDA would often fail to detect a signature, and if so, its LLDV would be volatile compared to the user-defined LLDV. The TDA, likewise, exhibited nearly no relationship to the tornado EF-scale or the user-defined LLDV.

4.1 General Relationships

For all scans utilized, there is an increase of the median of all user-defined LLDVs as EF-scale rating increases. However there is significant overlap amongst adjacent EF-scale ratings (Fig. 8) except for between EF2 and EF3. Most of the distributions for each EF-scale rating appear to be right-tailed. The EF4-5 distributions appear almost symmetric. One possible reason may be that EF4 damage has occurred with a variety of tornado widths and therefore, some tornado parent circulations may have been relatively poorly resolved. In this list of cases it is interesting to note that a user-defined LLDV > 65 ms^{-1} (85 ms^{-1}) implies a 75% (95%) chance respectively that the tornado is at least EF2 or greater.

For the MDA, the EF0 and EF1 tornadoes are combined due to the smaller sample size. However, similar to the user defined LLDV, the biggest separation in the middle 50% of values is between EF2 and EF3 (Fig. 9). In fact, there is no real separation amongst other adjacent EF-scale ratings. In this dataset, a MDA LLDV > 67 ms^{-1} is associated with 75% of cases

The TDA shows large overlap amongst all the EF-scale ratings except comparing EF0 to that of EF3 and above (Fig. 10). Above EF2, there is no substantial increase in the middle 50% of LLDV values.

4.2 Comparisons with tornado power

The question is whether or not the width of the tornado also influences the strength of the radar-based vortex signature? If so then perhaps some combination of tornado width and strength would have a stronger correlation with LLDV. Indeed, Wood and Brown (1997) demonstrated the increase in Delta-V occurred as the ratio of the vortex diameter to beam width increased. Thus if a vortex remained at constant range increasing its width resulted in a higher LLDV.

Estimating either the tornado kinetic energy or power dissipation provided the best method to incorporate both tornado width and intensity. We used power dissipation in preference over kinetic energy since it best reflected the amount of work done on the surface, and therefore, damage potential. This concept is similar to the Power Dissipation Index (PDI) proposed by Emanuel (2005) or the Hurricane Hazard Index (HHI) proposed by Kantha (2006), both applied to tropical cyclones. The relationship

$$P_{tor} = \frac{\pi \rho C_D \overline{V}^3 r^2}{4} \qquad 1)$$

represents the estimated power dissipation of the tornado, P_{tor} , where air density is ρ, surface drag coefficient is C_D, mean wind velocity is V, and radius of the ≥EF0 damage is r. Air density is set to standard atmosphere of 1.2 kg m^{-3}. C_D can vary dramatically from the order of 10^{-3} over the ocean (Emanuel, 2005) to 10^{-2} in deciduous forests (Mahrt et al. 2001). We set this value to 10^{-2} in order to focus on the meteorological relationship between tornado power and LLDV over terrain of constant roughness. The mean velocity, v, was estimated from the average of the mid-range values of the maximum EF-rating to a mid-range velocity value of the EF0 rating. The exception is that an EF5 rating converted to a lower bound wind speed of 90 ms^{-1}.

When the estimated power dissipation is compared with user defined LLDV, we find that there is an exponential upward trend, though with significant scatter (Fig. 11). Fitting an exponential regression reveals a correlation of 0.46. This is higher than the 0.4 correlation found by the EF-scale rating vs. user defined LLDV. For the MDA and TDA the correlation fell to 0.22 and 0.12 respectively. The improvement in correlation is an encouraging signal that power dissipation is a promising metric by which to compare with radar-derived vortex signature strength metrics.

4.3 Location errors

The user-defined vortex locations were predominantly located within the damage path of a tornado and had a median distance of ~300 m from the axis of greatest damage (Fig. 12). On the other hand, the median distance of the MDA was nearly 2 km and was often located completely outside of the damage path. The TDA improved upon the MDA in location with a median error of ~1 km. We note that the MDA was not designed to track the location of the tornado-like vortex signature.

5. DISCUSSION

The results show that while the correlation between user-defined LLDV and either EF-scale rating or tornado power dissipation rate is somewhat weak, it is much better than expected. Certainly issues remain that prevent better results. If one lesson can come from this is that the authors had to adjust the surveys on more than one occasion. Fortunately the high-resolution surveys and aerial imagery contain enough evidence to correct a majority of errors. However the problems don't go away because the EF-scale itself has numerous flaws, especially with vegetation. There are better methods for determining EF-scale ratings such as using vegetation blowdown patterns (eg, Beck and Dotzek, 2011), mobile Doppler radar (Wurman and Alexander, 2005 and Toth et al. 2011), and improved damage indicator guidance (Edwards et al. 2010).

Beam registration, or beam offsets still affect the vortex signatures. Assuming that the trends in this dataset continue with further analysis, MDA and TDA are inadequate to the task of real-time tornado intensity estimations unless velocity dealiasing is greatly improved. User-defined vortex diagnosis holds more promise but velocity differences are inherently more volatile than diagnostic methods involving integration (e.g., mesocyclone strength index, Stumpf et al. 1998).

Alternative vortex diagnostic algorithms hold promise in improving tornado power estimations. One technique converts radial velocity attributes into rotational kinetic energy and power using the modified Rankined combined vortex model (Desrochers and Donaldson, 1992). Newer techniques include one by Potvin et al. (2011) where they developed a variational method of fitting Dual Doppler velocities to an idealized vortex model from which diagnostics like strength can be derived. This approach can be used with single Doppler velocity data too. The linear least squares derivative approach to generating azimuthal shear (Smith et al. 2004) is also a promising avenue due to its resilience against beam sampling artifacts and its ability to use multiple radar data thereby improving sampling (Lakshmanan et al. 2006). In fact, Labriola et al. (2012) made an initial investigation on its capability of discriminating tornado intensity. Their results were inconclusive unless the width of the strong shear was accounted.

This last result appears to reinforce the idea that simply relating vortex diagnostic attributes to EF-scale rating alone is not sufficient. The better approach suggests that since radar vortex intensity is a result of both vortex strength and size, an energy, or power-based vortex set of attributes should be matched to equivalent attributes in the observations. Such a combination would appear to also be quire relevant to impact-based warnings since an impact of a tornado is not just related to its intensity but its size. Both attributes are related as Brooks (2004) has indicated. But there is also considerable variability in the size vs. strength relationship and thus both need to be accounted for based on high-resolution surveys.

All that has been discussed so far involves velocity-based tornado intensity estimation. With the advent of polarimetric WSR-88D capability, attributes of tornado debris (e.g., Bodine et al. 2012) will be of immense help to not only detect tornadoes but also to estimate tornado power when they are combined with velocity data.

6. CONCLUSIONS

In summary we have related user-defined and algorithmic WSR-88D vortex signature strengths from individual times to that of observed tornado intensity from high-resolution damage surveys. There are enough positive results to encourage us to continue pursuing a relationship between tornado power and the values of radar-based vortex diagnostics. However the dealiasing issues hurt the relationship between the algorithm-based LLDV from the MDA and TDA, and that of the EF-scale. This problem reinforces the need for human warning forecasters to evaluate the vortex signature strengths; however they need to become adept at correcting velocity dealiasing errors. Also important is improving ground-truth surveys. There is an ever greater need to have quality high resolution surveys if the NWS wants to produce quality impact-based tornado warnings.

Finally for new avenues of investigation, new samples will include some information about polarimetric debris signatures. New algorithms based on matching idealized vortex models, and the linear least squares derivative product, is also promising because their nature should help diminish the impact of scan-to-scan changes in vortex sampling by radar.

5. REFERENCES

Beck, V., N. Dotzek, 2010: Reconstruction of near-surface tornado wind fields from forest damage. *J. Appl. Meteor. Climatol.*, **49**, 1517–1537.

Bodine, D. J., M. R. Jumjian, R. D. Palmer, P. L. Heinselman, A. V. Ryzhkov. 2012: Tornado damage estimation using polarimetric radar, Wea. Forecasting, accepted. [Avaible online at http://journals.ametsoc.org/doi/abs/10.1175/WAF-D-11-00158.1]

Brooks, H. E., 2004: On the relationship of tornado path length and width to intensity. *Wea. Forecasting*, **19**, 310–319.

Brown, R.A., B. A. Flickinger, E. Forren, D.M. Schultz, D. Sirmans, P. L. Spencer, V.T. Wood, C. L. Ziegler, 2005: Improved detection of severe storms using experimental fine-resolution wsr-88d measurements. *Wea. Forecasting*, **20**, 3–14.

Brown, T. M. (2010). Development of a statistical relationship between ground-based and remotely-sensed damage in wind storms. Ph.D. Dissertation, Texas Tech University, 451 pp. [Available online at http://repositories.tdl.org/ttu-ir/handle/2346/45185]

Bunkers, M. J., and M. A. Baxter, Radar tornadic debris signatures on 27 April 2011. *Electronic J. Operational Meteor.,* **12** (7), 1-6. [Available online at http://nwas.org/ej/2011-ION1/]

Burgess, D. W., M. A. Magsig, J. Wurman, D. C. Dowell, Y. Richardson, 2002: Radar Observations of the 3 May 1999 Oklahoma City Tornado. *Wea. Forecasting*, **17**, 456–471.

Desrochers, P. R., R. J. Donaldson, 1992: Automatic tornado prediction with an improved Mesocyclone-Detection Algorithm. *Wea. Forecasting*, **7**, 373–388.

Edwards, J. G. LaDue, J. T. Ferree, K. A. Scharfenberg, C. Maier, W. L. Coulbourne, 2010: The Enhanced Fujita Scale: Past, present and future. Preprints, 25th Conf. Severe Local Storms., Amer. Meteor. Soc., Denver, CO, 4A.1. [Available online at:

https://ams.confex.com/ams/25SLS/webprogram/Paper175400.html]

Emanuel, K., 2005: Increasing destructiveness of tropical cyclones over the past 30 years. *Nature,* **436,** 686–688.

Hudson, M. J., P. A. Browning, K. Harding, K. J. Galluppi, and J. L. Losego, 2012: Central Region impact based warnings demonstration: a Weather-Ready Nation Initiative, 37th National Wea. Assoc. Meeting, Madison, WI, P2.4 [Available online at http://nwas.org/meetings/nwa2012/presentations/NWA2012_P2.40_Hudson_etal.zip]

Hudson, M. J., P. A. Browning, K. Harding, K. J. Galluppi, and J. L. Losego, 2012: Early findings and results from the Central Region Impact Based Warnings Demonstration, 37th National Wea. Assoc. Meeting, Madison, WI, D10.2 [Available online at http://nwas.org/meetings/nwa2012/presentations/NWA2012_D10.2_Hudson_etal.zip]

Kantha, L., 2006: Time to replace the Saffir-Simpson Hurricane Scale? *Eos, Trans. Amer. Geophys. Union,* **87,** 3–6.

Kingfield, D. M., J. G. LaDue, and K. L. Ortega, 2012: An evaluation of tornado intensity using velocity and strength attributes from the wsr-88d mesocyclone detection algorithm. Preprints, 26th Conf. Severe Local Storms. Amer. Meteor. Soc., Nashville, TN. 3.2 [Available online at: https://ams.confex.com/ams/26SLS/webprogram/Paper211488.html]

Labriola J., K. L. Ortega, D. M. Kingfield, and M. L. Miller. 2013: Investigating the relationship of multi-radar multi-sensor parameters to tornado intensity, 12th Annual Student Conference, Austin, TX, Amer. Meteor. Soc., S118.

Lakshmanan, V., T. Smith, K. Hondl, G. J. Stumpf, A. Witt, 2006: A real-time, three-dimensional, rapidly updating, heterogeneous radar merger technique for reflectivity, velocity, and derived products. *Wea. Forecasting*, **21**, 802–823.

Mahrt, L., D. Vickers, J. Sun, N. Otto Jensen, H. Jorgensen, E. Pardyjak, and H. Fernando, 2001: Determination of the surface drag coefficient, *Boundary-Layer Meteorology*, **99**, 249-276.

Mitchell, E. D., S. V. Vasiloff, G. J. Stumpf, A.Witt, M. D. Eilts, J. T. Johnson, K. W. Thomas, 1998: The National Severe Storms Laboratory Tornado Detection Algorithm. *Wea. Forecasting*, **13**, 352–366.

NOAA, 2007: National Weather Service instruction 10-1605: Storm data preparation. [Available online at http://www.nws.noaa.gov/directives/sym/pd01016005curr.pdf]

NOAA, 2011a: NOAA NWS operations and services during the historic tornado outbreaks of April 2011, 76 pp [Available online at: https://verification.nws.noaa.gov/sats/sa.aspx?id=12]

NOAA, 2011 b: May 22, 2011 Joplin Tornado (Regional Service Assessment) [Available online at: https://verification.nws.noaa.gov/sats/sa.aspx?id=22]

Potvin, C. K., A. Shapiro, M. I. Biggerstaff, J. M. Wurman, 2011: The VDAC technique: A variational method for detecting and characterizing convective vortices in multiple-doppler radar data. *Mon. Wea. Rev.*, **139**, 2593–2613.

Smith, B. T., R. L. Thompson, H. E. Brooks, A. R. Dean, and K. L. Elmore. 2012: Diagnosis of conditional maximum tornado damage probabilities, Preprints, 26th Conf Severe Local Storms, Nashville, TN, Amer. Meteor Soc., P2 20, [Available online at https://ams.confex.com/ams/26SLS/webprogram/Paper211807.html]

Smith, T.M. and K. L. Elmore, 2004: The use of radial velocity derivatives to diagnose rotation and divergence. Preprints, 11th Conf. on Aviation, Range, and Aerospace, Hyannis, MA, Amer. Meteor. Soc., P5.6 – CD preprints.

Speheger, D. A., Charles A. Doswell, G. J. Stumpf, 2002: The Tornadoes of 3 May 1999: Event verification in central oklahoma and related issues. *Wea. Forecasting*, **17**, 362–381.

Stefkovich, J., T. P. Marshall, J. De Block, J. G. LaDue, and C. Karsten, 2012: Damage survey of the Tuscaloosa – Birmingham, AL tornado. Preprints, 26th Conf of Severe Local Storms, Nashville, TN, Amer. Meteor. Soc., P5.3.

Stellman, K. and P. Camp, 2012: D9.2 The Storm Damage Assessment Toolkit - Storm Damage Survey Data Collection using Smartphones and Tablets. NWA Annual Meeting, Madison, WI. Natl. Wea. Assoc., D9.2. [Available online at: http://nwas.org/meetings/nwa2012/presentations/NWA2012_D9.2_Stellman_Camp.zip]

Stumpf, G. J., A. Witt, E. D. Mitchell, P.L. Spencer, J. T. Johnson, M. D. Eilts, K. W. Thomas, D.W. Burgess, 1998: The National Severe Storms Laboratory Mesocyclone Detection Algorithm for the WSR-88D*. *Wea. Forecasting*, **13**, 304–326.

Torres, S. M., and C. D. Curtis, 2007: Initial implementation of super-resolution data on the NEXRAD network, preprints, 23rd Conf. Interactive Information Processing Systems, San Antonio, TX, 5B.10.

Toth, M., R. J. Trapp, J. Wurman, and K. A. Kosiba 2011: Enhancing tornado intensity estimates with Doppler radar., Preprints, 35th Conf. on Radar Meteorology, Pittsburg, PA., 4B.1. [Available online at https://ams.confex.com/ams/35Radar/webprogram/Paper191315.html]

Wood, V. T., and R. A. Brown, 1997: Effects of radar sampling on single-doppler velocity signatures of mesocyclones and tornadoes. *Wea. Forecasting*, **12**, 928–938.

WSEC, 2006: A recommendation for an enhanced Fujita scale (EF-scale). Wind Science and Engineering Center, Texas Tech University, Lubbock, Texas, 95 pp. [Available online at http://www.depts.ttu.edu/weweb/EFScale.pdf

Wurman, J., C. R. Alexander, 2005: The 30 May 1998 Spencer, South Dakota, Storm. Part II: Comparison of observed damage and radar-derived winds in the tornadoes. *Mon. Wea. Rev.*, **133**, 97–119.

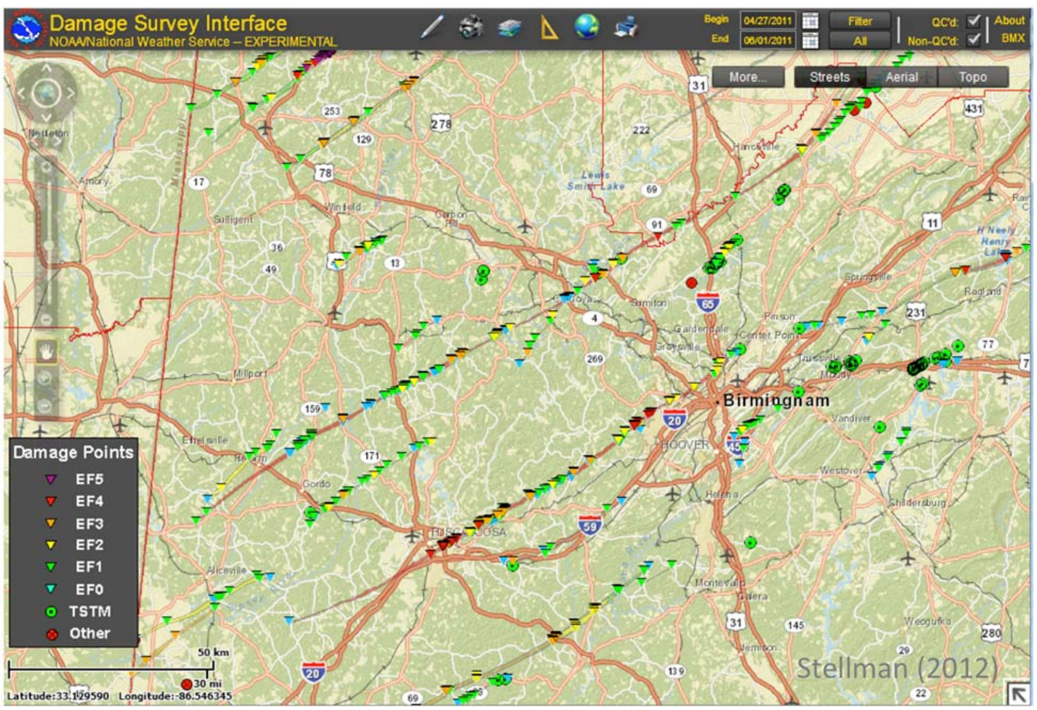

Figure 1 The depiction of multiple high resolution tornado surveys from 2012 April 27 visualized in the Damage Assessment Toolkit (DAT). The individual triangles are color coded by EF-scale. Some tornado tracks are contoured by EF-scale ratings

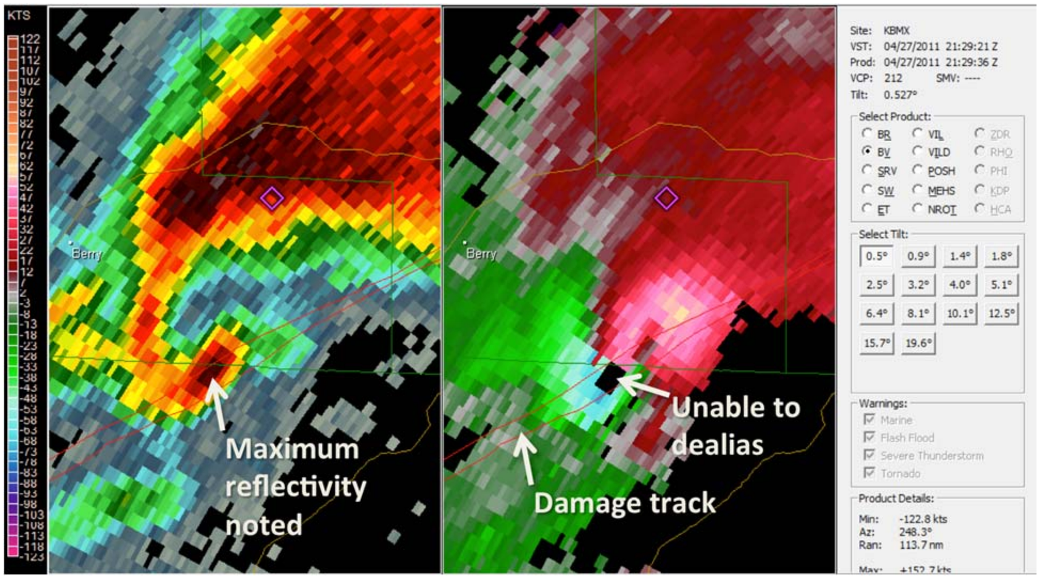

Figure 2. Similar to figure 2 except the raw radial velocity is displayed. V_{max} and V_{min} depict the velocity extrema used in the LLDV. The outer V_{max} was not considered because of its distance from the tornado at the scan time.

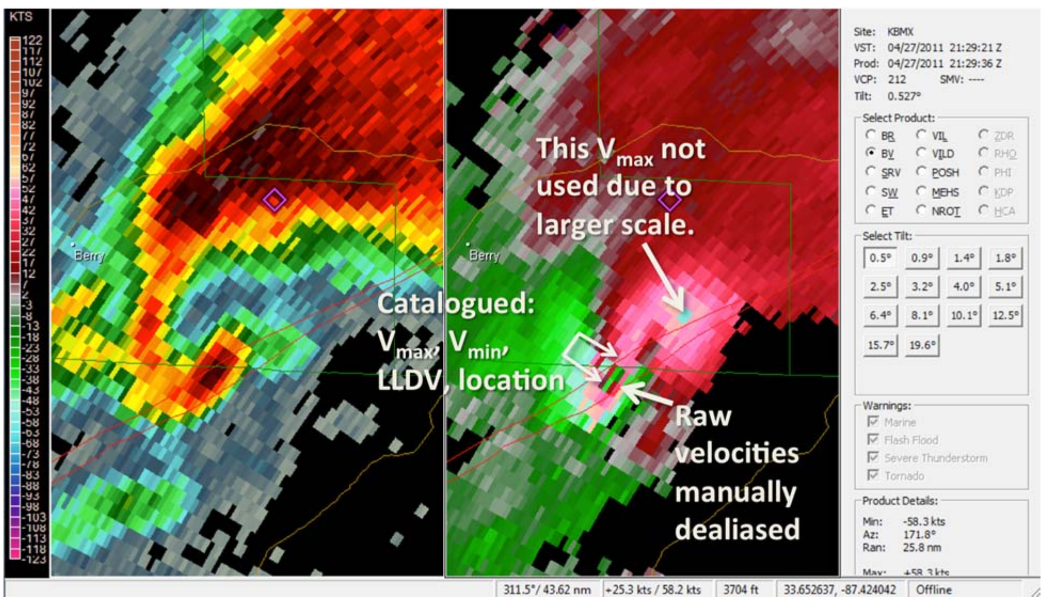

Figure 3 The KBMX lowest scan reflectivity (left panel) and radial velocity (right panel) depicting the Reform to Cordova, AL, tornado on 2012 April 27 2129 UTC. The EF0 contour of the tornado damage track appears in red. The label 'unable to dealias' refers to the difficulty of the Gibson Ridge GRlevel2 analyst software to dealias the velocity.

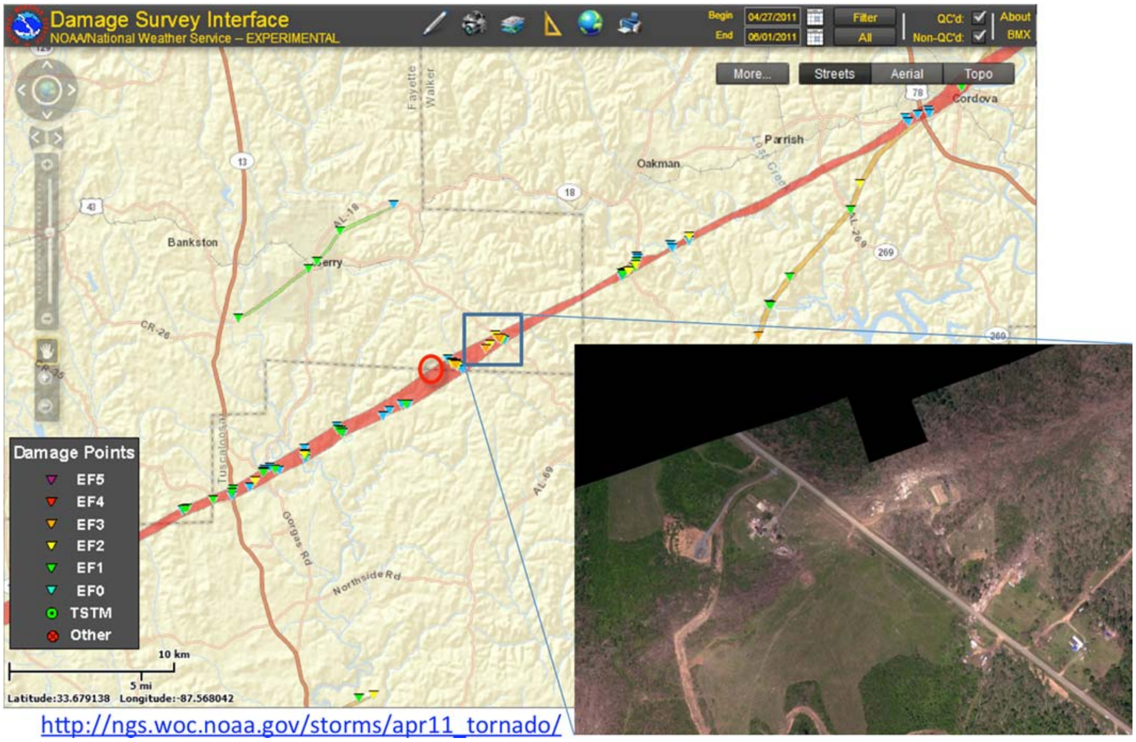

Figure 4. A DAT display of the Reform to Cordova, AL, tornado of 2011 April 27. The orange swath encompasses the ≥EF0 damage. Individually rated Damage Indicators (DI) appear as triangles colorcoded by EF rating following the legend (left). The red circle indicates the location of the vortex signature observed from KBMX at 2129 UTC (Figs 2 and 3). The blue box appears to represent the inset aerial image of the damage track used to verify the ground-based ratings.

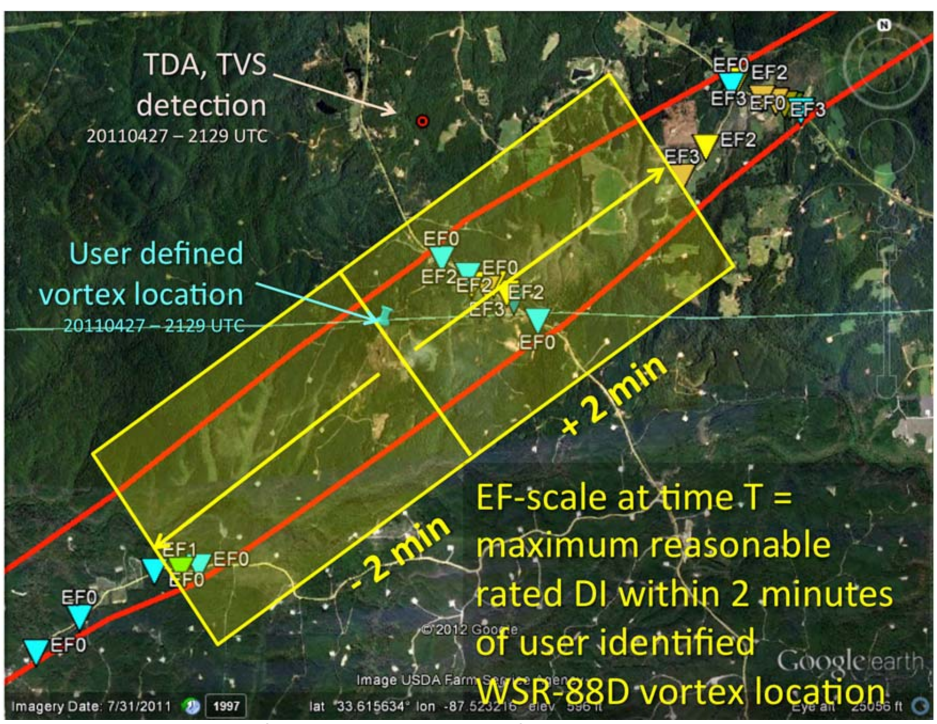

Figure 5. A schematic of the temporal window of ±2 min converted to a spatial window (yellow box) assuming a vortex motion of 25 ms^{-1} parallel to the damage track (red contour). The spatial window is centered at the position of the radar identified vortex signature shown in figures 2 and 3.

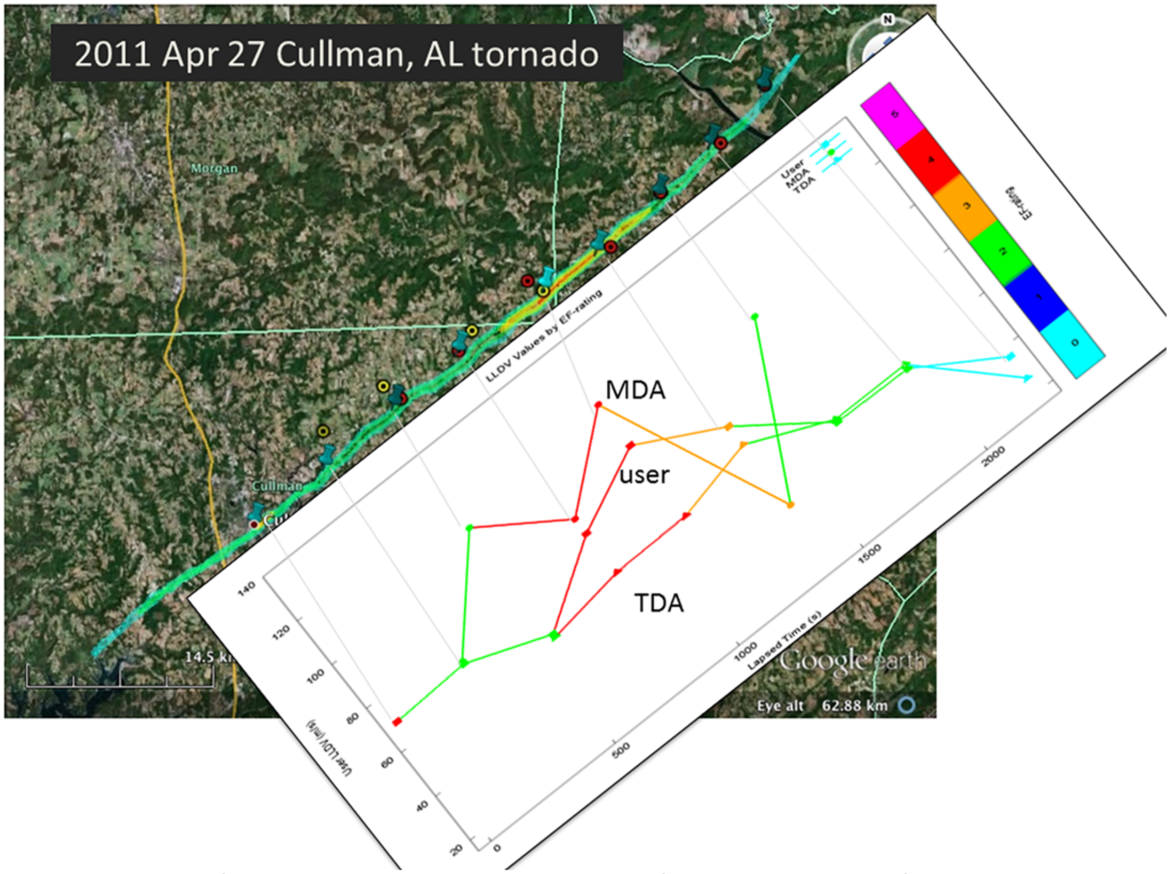

Figure 6. A display of the EF-scale contoured map shows the Cullman, AL, tornado of 2011 April 27. The contours are colored blue for EF0-1, green for EF2, yellow for EF3, and red for EF4. In the map, the blue pin cushions represent the user-based WSR-88D vortex signature locations where the brightness is related to LLDV. The yellow circles represent the MDA locations color-coded by LLDV and the red circles are TDA detections. The chart shows the LLDV values in a timeline for the user-defined, MDA, and TDA detections. The grey lines link the detection times in the chart to the locations on the map. The traces in the chart are color coded by EF-scale where the legend is on the right side.

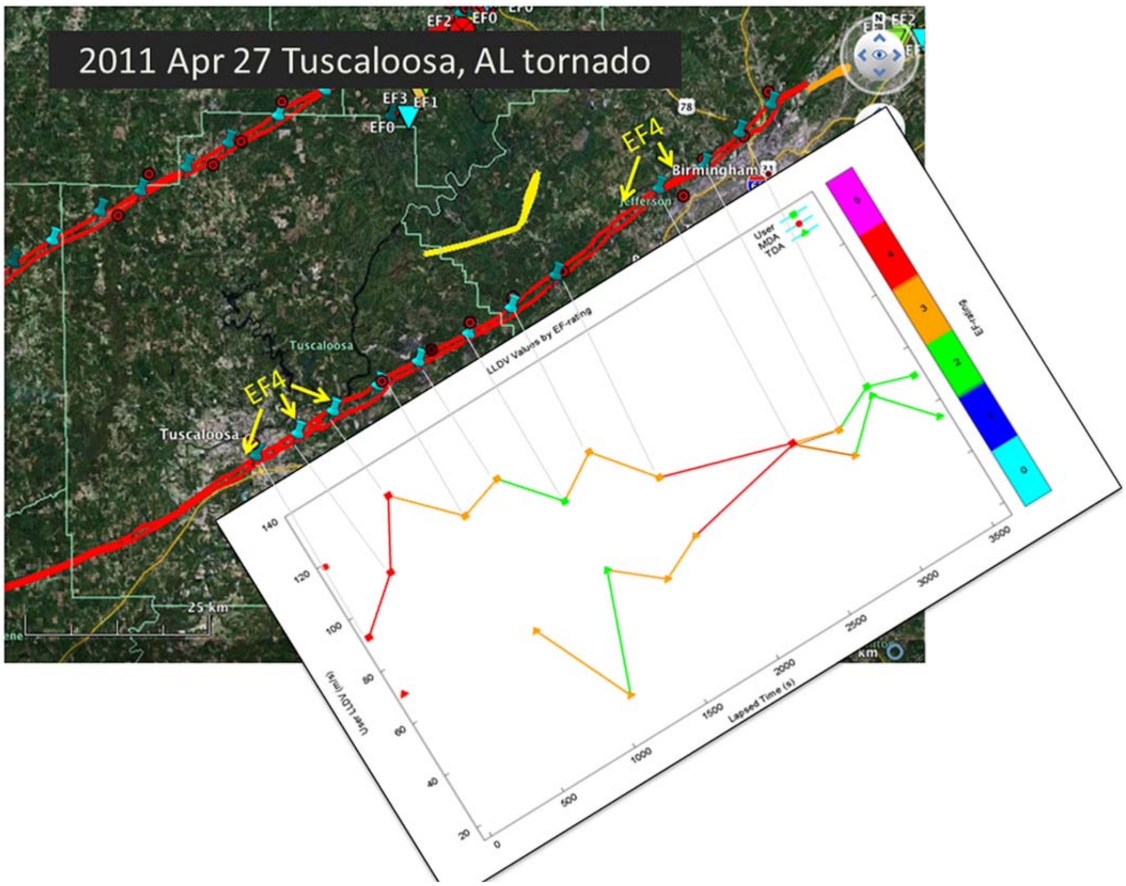

Figure 7. This tornado track map is similar to figure 6 except for the Tuscaloosa, AL, tornado from 2011 April 27. The MDA detections are missing and only the EF0 damage contour appears. However segments with EF4 damage are labeled on the map.

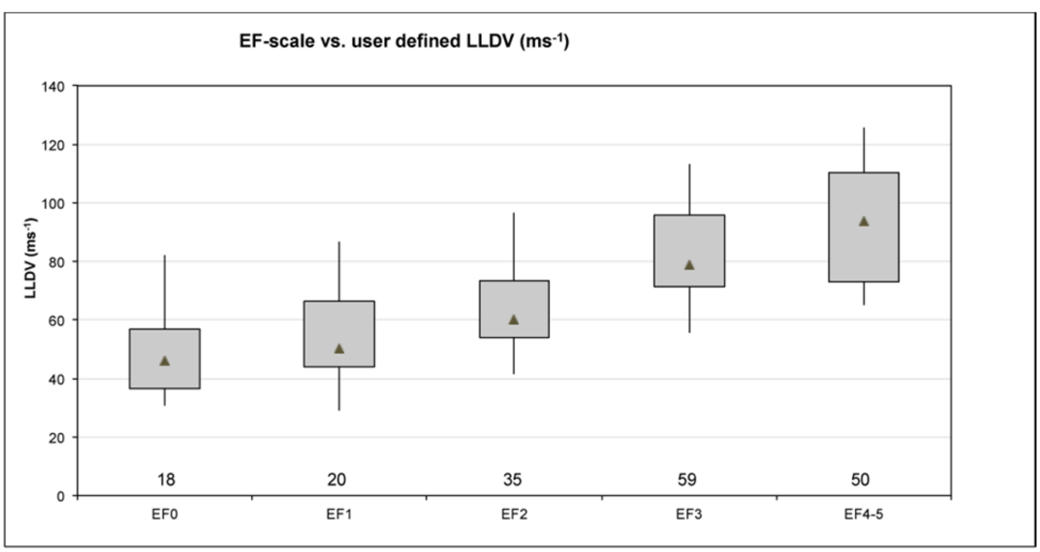

Figure 8. Box and Whiskers plot of user defined LLDV vs EF-scale rating. The bottom and the top of the whiskers represent the 5 and 95 percentiles respectively while the box represents the middle 75% of values. The triangles represent the median values. The numbers along the x-axis represents the numbers of detections in each EF-scale rating.

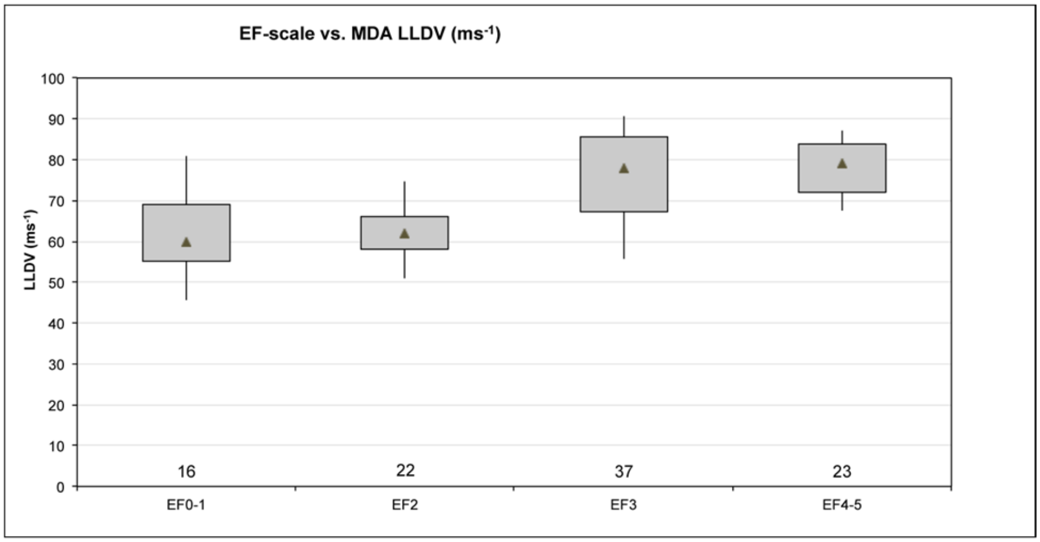

Figure 9. Similar to figure 8 except for MDA LLDV.

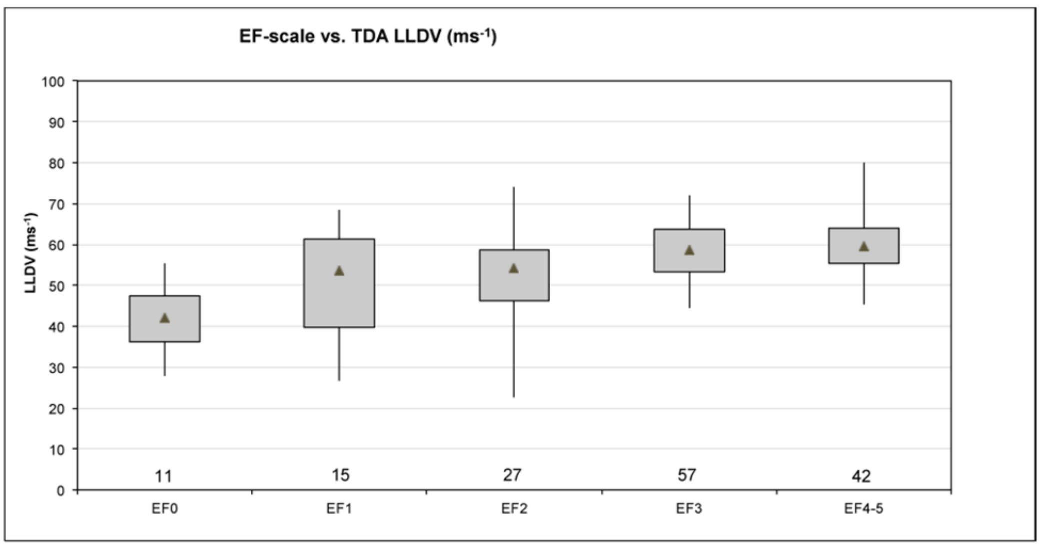

Figure 10. Similar to figure 8 except for the TDA LLDV.

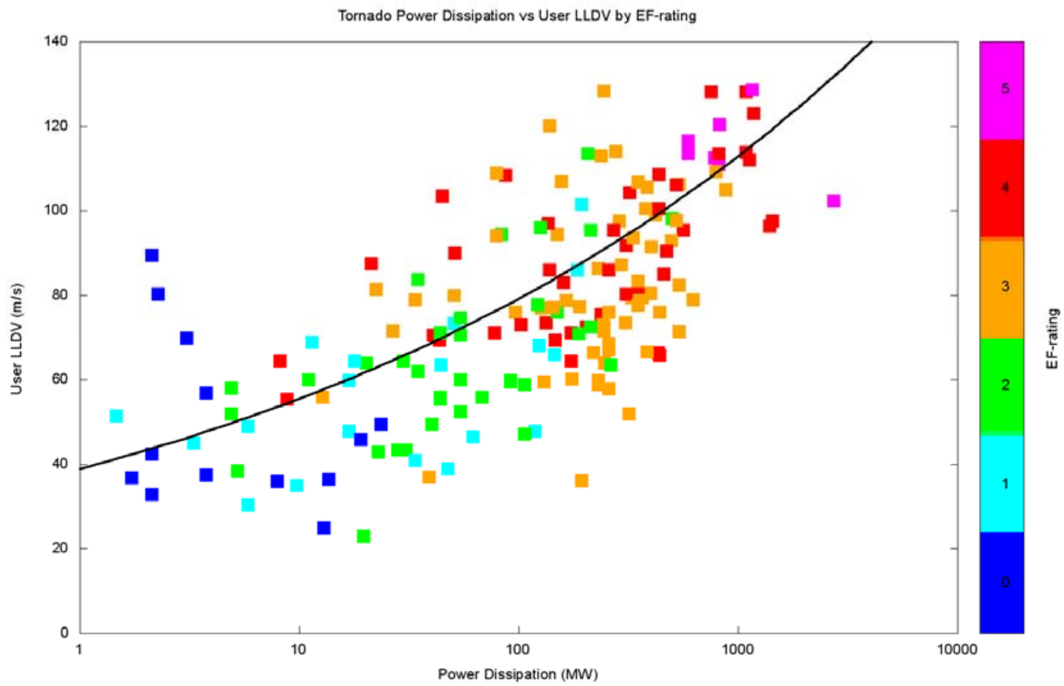

Figure 11. A scatterplot of tornado power dissipation as a function of user defined LLDV. The thin dark curve represents the best-fit representing a correlation of 0.46. The individual detections are color coded by EF-scale rating.

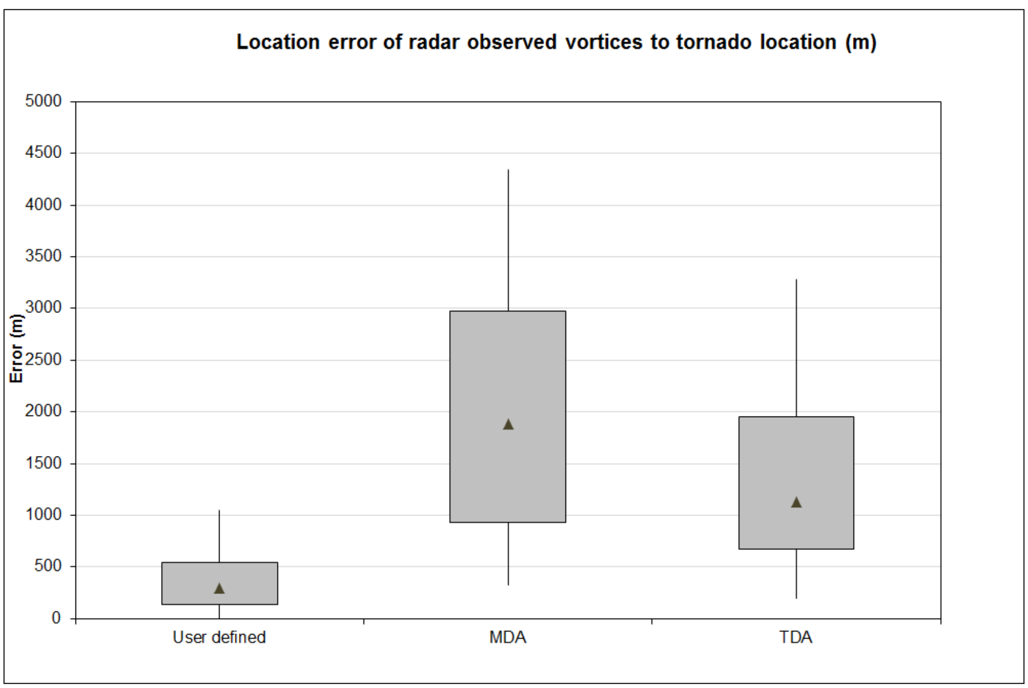

Figure 12. This plot shows the location errors of radar-based vortex locations relative to the closest point of the strongest tornado damage. The values of the box and whiskers plot are similar to figure 8.

Table 1. This table represents a list of tornadoes used in this study. The initial sampling time refers to the first time a user-defined vortex was identified in conjunction with high-resolution ground survey information. The number of scans represents all WSR-88D lowest elevation scans sampling each tornado to identify a user-defined vortex signature associated with a tornado. The number of TDA and MDA detections per tornado represents the total number of matches with the user-base signature detections. The maximum EF-scale represents the highest value found per tornado when a user-defined vortex signature was identified. The asterix (*) in the EF-scale column indicates that the tornado had a higher rating (EF5) outside the time of the user-defined vortex locations.

Tornado ID	Date	Initial sampling time (UTC)	Number of scans	Number of TDA detections	Number of MDA detections	Maximum EF-scale	Storm type
Cordova, AL #1	27-Apr-11	1017	4	0	3	3	QLCS
Hoover, AL	27-Apr-11	1054	2	1	2	1	QLCS
Cullman, AL	27-Apr-11	1956	9	7	0	4	RM
Cordova, AL #2	27-Apr-11	2057	20	17	8	4	RM
Smithville, MS	27-Apr-11	2101	5	4	5	3* (5)	RM
Tuscaloosa, AL	27-Apr-11	2210	12	10	1	4	RM
Haleyville, AL	27-Apr-11	2219	5	4	4	3	RM
Sawyerville, AL	27-Apr-11	2255	13	12	10	3	RM
Margaret, AL	27-Apr-11	2332	8	7	6	4	RM
Joplin, MO	22-May-11	2234	8	6	4	5	RM
El Reno, OK	24-May-11	2053	48	46	26	5	RM
Blanchard, OK	24-May-11	2208	25	22	18	4	RM
Goldsby, OK	24-May-11	2230	16	14	8	4	RM
Blanchard, OK #2	8-Nov-11	445	1	0	0	1	QLCS
Norman, OK	13-Apr-12	2100	3	0	5	1	RM
total			179	150	100		